Determination of Transformer Winding Radial Deformation Using UWB System and Hyperboloid Method

Hesam Rahbarimagham, Hossein Karami Porzani, Maryam Sadat Akhavan Hejazi, Mahdi S. Naderi, and Gevork B. Gharehpetian, *Senior Member, IEEE*

***Abstract*— Online monitoring of the transformer winding using electromagnetic waves has recently been proposed for the detection of mechanical defects of transformer winding. In this paper, a new method, which uses the ultrawideband radar measurement results and is based on locus of objects in the space, is proposed for the 3-D positioning of transformer winding radial deformation location. The proposed experimental setup for this method named hyperboloid method is modeled using Computer Simulation Technology software. In this paper, Vivaldi antennas suitable for measurements in environments with multipath, are used and the analysis is performed in the time domain. The simulation results show that the exact 3-D location of the radial deformation can be detected with a good accuracy.**

***Index Terms*— Monitoring, radial deformation, power transformer winding, UWB system, hyperboloid method.**

I. Introduction

POWER transformers are the main elements of the transmission and distribution networks [1]. In industrial plants, mechanical damages such as radial deformations are caused by forces due to high short circuit currents [2]–[5]. The proper design, monitoring and investigation of the forces acting on the transformers are crucial [6], [7]. There are many transformer monitoring methods such as short circuit test method, frequency response analysis method and low voltage impulse test method [8]–[10]. The short circuit test method is based on measurement of the short-circuit reactance [11]–[13]. It can be performed on-line, simultaneously with the operation of the transformer, but does not provide any information about the type and location of the fault. The frequency response analysis method has been mentioned in the literatures as an on-line method, but only the high voltage winding of the transformer remains in the circuit [14], [15] and the low voltage winding of the transformer should be disconnected from the circuit. The low voltage impulse test method [16], [17] is also an off-line method, i.e. the transformer must be isolated from the network. The off-line methods will not meet all the needs of the transformer monitoring system but on-line methods have the benefit of the continuous monitoring of the power transformer winding. However, on-line Transfer Function using time domain or frequency domain [18], [19] has been introduced as on-line methods in order to real-time recognition of transformer winding deformation or displacement.

Recently, a new frequency domain method has been proposed based on scattering parameters measurement [20], [21]. This method is based on the measurement of the reflected signal which is sine sweep from the transformer winding. Mechanical damages can also be detected using time domain measurement of Ultra Wide Band (UWB) waves. In this method, the narrow pulses generated by the transmitting UWB radar system are emitted to the transformer and its reflection is stored. The information from the reflections can be utilized to study the condition of the winding by comparison [22] or image generation [23] methods. In [23], a method for an in-depth detection of the winding radial deformation is presented, providing details of the fault. This method is based on the synthetic aperture radar (SAR) imaging. The only demerit of this method is the need of the antenna movement.

The discussed approaches are reliable tool for the detection of the transformer winding displacement and deformation, but determining the extent of transformer winding deformation without considering its location leads to unreliable estimations [24]. This localization feature, although still in its infancy, makes this tool unique and worthy of further scrutiny. Driven by this motivation, recent progress about localization of transformer winding deformation using frequency-based technique has been presented [25]–[27].

In this paper, an analytical method is proposed to detect the transformer winding mechanical damages in the three-dimensional space by using Hyperboloid method. The proposed method is used to detect the exact location of the radial deformation based on locus of hyperboloids calculated by using reflected UWB signals. The signals used for this method have a high accuracy for the transformer winding deformation detection because of the excellent spatial

Manuscript received February 9, 2014; revised March 17, 2015; accepted March 18, 2015. Date of publication March 23, 2015; date of current version June 10, 2015. This work was supported by Tehran Regional Electric Company. The associate editor coordinating the review of this paper and approving it for publication was Dr. Lorenzo Lo Monte.

H. Rahbarimagham, H. K. Porzani, M. S. Naderi, and G. B. Gharehpetian are with the Center of Excellence on Power Systems, Department of Electrical Engineering, Amirkabir University of Technology, Tehran 15875-4413, Iran (e-mail: h.rahbarim@aut.ac.ir; h.karami@aut.ac.ir; salaynaderi@aut.ac.ir; grptian@aut.ac.ir).

M. S. A. Hejazi is with the Department of Electrical Engineering, University of Kashan, Kashan 87317-51167, Iran (e-mail: akhavanhejazi@gmail.com).

Color versions of one or more of the figures in this paper are available online at http://ieeexplore.ieee.org.

Digital Object Identifier 10.1109/JSEN.2015.2415554

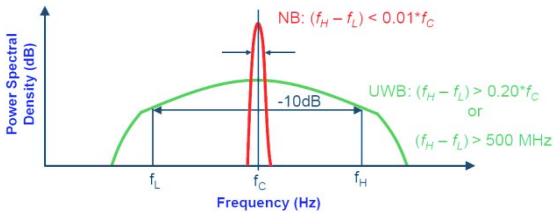

Fig. 1. Relative bandwidth of narrowband and broadband systems.

TABLE I
PARAMETERS OF THE TRANSMITTED PULSE

Center Frequency (radiated)	4.7GHz
Bandwidth (10 dB radiated)	3.2 GHz

resolution of the Ultra Wide Band system. The good quality of time resolution of UWB signals enables potential in high-resolution ranging [22]. One of the key advantages of the UWB is the ability to attain high spatial resolution and discriminate between targets in close proximity to each other. In this study, the CST software has been used to simulate the model of the winding displacement.

II. UWB Systems Application for Transformer Monitoring

According to established standards [28], UWB systems refer to systems that relative bandwidth used in them is more than a 0.2 (Fig. 1). The fractional bandwidth is defined by the following equation:

$$b = 2\frac{(f_H - f_L)}{(f_H + f_L)} \tag{1}$$

where, f_H is the *10dB* upper cut-off frequency and f_L is the $-10dB$ lower cut-off frequency. In Fig. 1, the center frequency is indicated by f_c.

In this study, transmitted UWB pulse is detailed in Table I. Fig. 8 shows a Gaussian pulse in time domain.

A UWB pulse is sent toward the transformer winding by a transmitting antenna. The part of the energy reflected from the transformer winding is received and stored by the receiving antenna. The main idea of this technique has been presented in [20]–[23]. The novelty of this paper is to propose an analytical method to determine the exact location of the transformer winding radial deformation. In this method, the locations of antennas are fixed. The solution presented in [23] needs the movement of antennas and cannot determine the exact location of deformation. Thus, this problem is solved by the proposed method of this paper. In [29] and [30], the two-dimensional hyperbolic method has been discussed. In this paper, the proposed method has been expanded for the three dimensional transformer winding radial deformation detection and determination. Comparison of the received signals in the time domain is performed using cross correlation method has been applied to analyze the received signals.

III. Radial Deformation Localization Using Hyperboloid Method

UWB sensor networks promise interesting landscape for localization in the short-range environment [31]. There are many existing localization methods by using UWB networks [32]–[35], such as angle of arrival (AOA), received signal strength intensity (RSSI), time of arrival (TOA) and time difference of arrival (TDOA). Among these methods, the ranged-based schemes, TOA and TDOA, are proved to have a very good accuracy [36] because of the large bandwidth of the UWB signals.

If a pulse is emitted from a platform, it will arrive at slightly different times for two spatially separated receiver sites, the TDOA being due to the different distances of each receiver from the platform. In fact, for given locations of the two receivers, a whole set of emitter locations would give the same measurement of TDOA. For given two receiver locations and a known TDOA, the locus of possible emitter locations is a one-half of a two-sheeted hyperboloid. In simple terms, for example two receivers at known locations, an emitter can be located onto a hyperboloid. The benefit of TDOA method vs. TOA method is that in TDOA method the receivers do not need to be synchronized with the transmitter [37].

This paper focuses on analyzing the received signals for the exact determination of the radial deformation location in the transformer winding. The radial deformation changes the UWB signal. In order to perform the test, four transmitting antenna and eight receiving antennas are used. Fig. 2 (a) shows the arrangement of antennas around the transformer. There are four sets of antennas in the test setup and each set (r_i) consists of three antennas: one transmitting antenna and two receiving antennas. Each set with other sets is 90 degrees apart. 180 degrees of the transformer model surface is screened by a set of antennas and two sets can see only 90 degrees of the surface simultaneously (Fig. 2 (c)). In each receiver, the signal of the sound condition is subtracted from the signal of the deformed condition which will be mentioned in the paper as subtracted signal. The differences of mentioned signals show whether the winding is defected or not?

In this paper, the three-phase transformer bank including 3 single-phase transformers is studied. This configuration is simple but the suggested solution can be applied to three-phase single core transformers as shown in Fig. 2 (e).

As shown in Fig. 2(d), if a deformation exists in the transformer windings, two receiving antennas in one set see the failure in different time intervals. t_1 and t_2 are the time difference between the peak of the subtracted signal from the time origin of transmitted signal, as shown in Fig. 3. It should be noted that in the background subtraction, the previously received signal is subtracted from the sound received signal. However, there is no need to be synchronized with the transmitted signal because the method is based on TDOA and not TOA. In the other words the advantage of this method is that the receiving antennas do not need to know the absolute time (t_1 and t_2) at which the pulse was transmitted and only the time difference ($t_1 - t_2$) is needed. While calculating the TDOA, it is not necessary to synchronize the received signal with that of transmitter. However, it should be noted that the

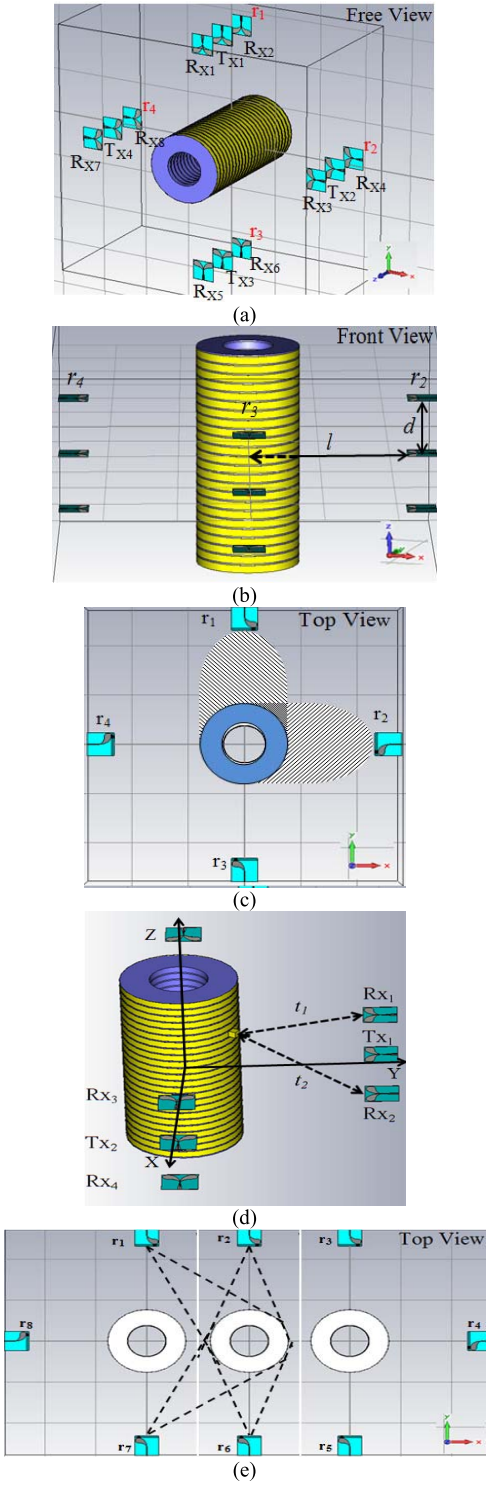

Fig. 2. Simulated system. (a) Three-dimensional view. (b) Front view. (c) Top view. (d) Time difference of signals received by a pair of receiver. (e) Three-phase design.

background signal and the received one should be necessarily synchronized to properly perform background subtraction. This synchronization can be obtained by matching the main peaks of both signals.

The signal propagation speed, which is the light speed, can be used to map the time interval to the distance difference

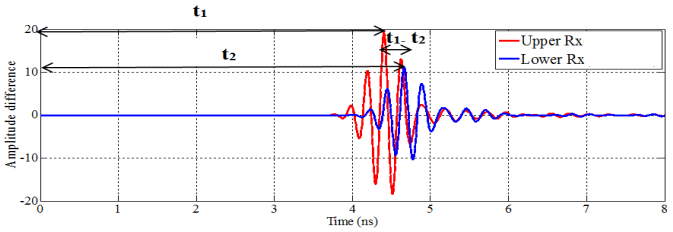

Fig. 3. Time difference of subtracted signals which received by a pair of receivers.

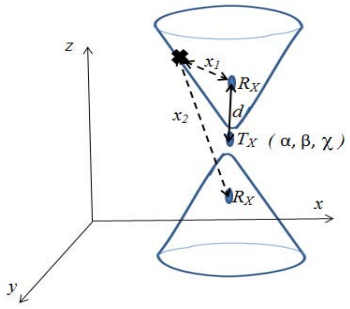

Fig. 4. Hyperboloid.

as follows:

$$x_1 - x_2 = (t_1 - t_2) \times v \tag{2}$$

where, v is equal to 3×10^8 m/s. In the above formula, x_1 and x_2 are the distances of first and second receiving antennas from the defection, respectively.

Thus, for a certain radial deformation, the distance difference from two fix points (receiving antennas) can be obtained. The locus of the deformation location is obtained considering the fact that the locus of points with constant difference of distance from two fix points is a hyperboloid with receiving antennas as its foci. The equation of the hyperbola can be written as follows:

$$\frac{(z-\alpha)^2}{a^2} - \frac{(x-\beta)^2}{b^2} - \frac{(y-\chi)^2}{c^2} = 1 \tag{3}$$

where, $2a$ is the difference of the distance of points on the hyperboloid from hyperboloid foci (receiving antennas) as follows:

$$2a = x_1 - x_2 \tag{4}$$

The parameters α, β and χ are the coordinate of symmetry points of the hyperboloid. The parameters b and c are calculated using the following equation:

$$b^2 = c^2 = d^2 - a^2 \tag{5}$$

where, d is the distance from the center (transmitting antenna) to either focus point (receiving antennas) of the hyperboloid as shown in Fig. 4. It should be noted that a is obtained using the analysis of received signals explained in section IV.

An unknown deformation location in the coordinate (x_0, y_0, z_0) can be determined by simultaneous solution of three equations. One of the equations is the equation of the cylinder surface, as the surface of the transformer is the locus

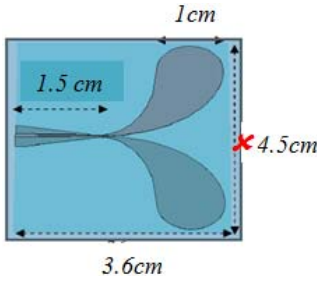

Fig. 5. Structure of Vivaldi antenna.

TABLE II
COORDINATES OF ANTENNAS LOCATION FOR DETECTION OF DEFORMATION IN FIRST QUADRANT

Set of antennas	Upper receiving antenna(x,y,z)	Transmitting antenna(x,y,z)	Lower receiving antenna(x,y,z)
r_1	R_{X1}:*(0,l,d)*	T_{X1}:*(0,l,0)*	R_{X3}:*(0,l,-d)*
r_2	R_{X2}:*(l,0,d)*	T_{X2}:*(l,0,0)*	R_{X4}:*(l,0,-d)*

of the deformation location. It should be noted that each deformation on the winding surface is seen by two sets of antennas simultaneously (Fig. 2(c)). Consequently, two hyperboloids equations are obtained. If the deformation location is considered in the first quadrant of the coordinate (i.e., x, y>0), as shown in Fig. 2(d), the cylinder and hyperboloid equations can be derived as follows:

$$x^2 + y^2 = r^2, \quad -30cm < z < +30cm \tag{6}$$

$$\frac{z^2}{a_0^2} - \frac{(x-l)^2}{b_0^2} - \frac{y^2}{c_0^2} = 1 \tag{7}$$

$$\frac{z^2}{a_1^2} - \frac{x^2}{b_1^2} - \frac{(y-l)^2}{c_1^2} = 1 \tag{8}$$

where, l is the distance between transformer winding center and transmitting antenna location and r is the transformer winding model radius. All of the parameters are shown in Fig. 2. a_0, b_0, c_0, a_1, b_1 and c_1 are calculated using the equations (4) and (5). The coordinates of the antennas location in the adopted test system which is indicated by a red cross in Fig. 5, are given in Table II.

The deformation location is obtained by solving the equations (6), (7) and (8). In other words, an intersection of two hyperboloids and one cylinder detects the exact location of the deformation. Two hyperboloids with the cylinder (transformer winding surface) have four common points. Two points that are located near the antennas are acceptable. From these two points, the one which is near to the antenna that detects the signal difference first, is the acceptable point.

The hyperboloid algorithm can be summarized as follows:

Step 1: Sending and receiving signals for sound and defective conditions of the transformer are stored.

Step 2: For each set of antennas, the sound condition signals are subtracted from the defect one.

Step 3: The two sets of antennas which detect the defection is identified.

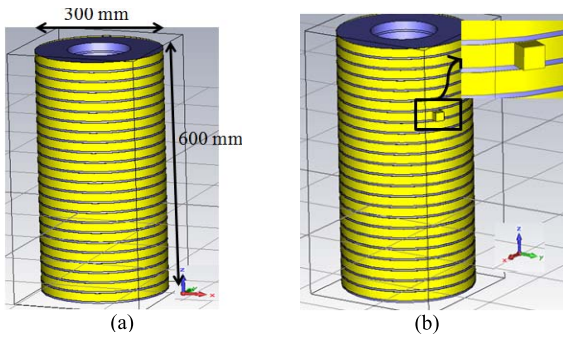

Fig. 6. Simulated transformer winding. (a) Normal mode of transformer. (b) Defected mode.

TABLE III
TRANSFORMER MODEL PARAMETERS

Phase number	1
Space between disks	5 mm
Number of disks	24
Height	600 mm
Outer diameter	300 mm

Step 4: The quadrant in which the defection exists is determined.

Step 5: The time difference of subtracted signals for two receiving antennas has been determined by cross correlation method. The peak of the cross-correlation of two "subtracted signals" is the criteria for (approximate) time difference.

Step 6: The obtained time difference is mapped to the distance using the signal propagation speed.

Step 7: Two hyperboloid equations as the locus of the deformation location are obtained from two sets of antennas positions.

Step 8: The surface of the transformer winding is considered as a cylinder.

Step 9: The location of the radial deformation is determined considering the intersection of two hyperboloids and the cylinder (drawing of the winding from the manufacturer).

IV. SYSTEM MODELING

The modeled set-up has two parts:

- Transformer winding
- Vivaldi antenna.

A. Transformer Winding Model

Due to the complexity of the transformer, the utilized model for the simulation is relatively simple and smaller in size and neglects the tank and the oil effect for single-phase case. As shown in Fig. 6(a), this model consists of a cylinder with layers of copper. The dimensions of the simulated model are given in Table III.

It should be noted that the UWB pulses are completely reflected from the copper, so there is no need to model inside of the transformer winding. To model the radial deformation, a metal sector with a width of 2cm on transformer winding has been modeled as shown in Fig. 6 (b). It should be noted

TABLE IV
SYSTEM PARAMETERS

l	550 mm
d	150 mm
r	150 mm

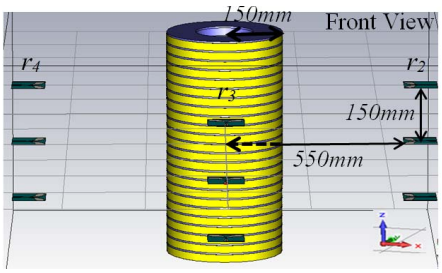

Fig. 7. Simulation setup with dimension of components.

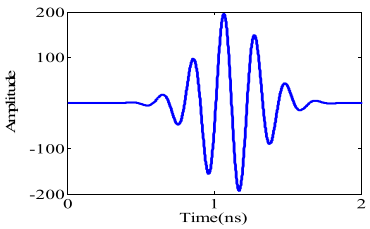

Fig. 8. A sample of transmitted signal.

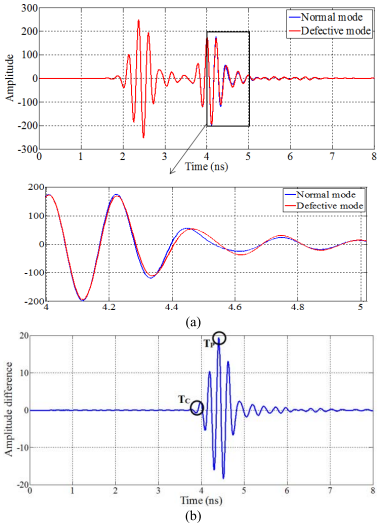

Fig. 9. A sample received signals by receiving antennas. (a) Normal and defective mode of transformer and (b) difference of signals in normal and defective modes.

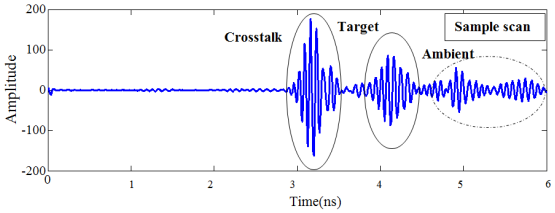

Fig. 10. Components of a sample scan.

that in order to implement Hyperboloid method in an actual transformer, a window should be installed on the transformer tank [22], [23].

B. Vivaldi Antenna Model

In this paper, Vivaldi antenna as one of the most reliable and suitable antennas for UWB applications, is simulated. The antenna frequency band is from 3.2 GHz to 6.2 GHz. The antenna structure and its dimensions are shown in Fig. 5.

Short duration of the ringing, the high peak value and the narrow width of the pulses and stable group delay are the many advantages of the Vivaldi antenna; and those are the essential requirements for the UWB pulse radar. The measurements show that the ringing duration of the Vivaldi UWB antennas is short and the main pulse widths are narrow, which underlines the accuracy of the test antenna [38], [39].

V. SIMULATION RESULTS

In this section, the proposed method is applied to detect the radial deformations in two different locations. The parameters of the simulated system shown in Fig. 2(b), are given in Table IV. An overview of simulation setup with dimension of components is shown in Fig. 7.

The model of the transformer winding in sound condition (i.e., winding without buckling) is simulated. In this mode, sending and receiving signals are performed by Vivaldi antennas; and the data are stored. The signal profile is shown in Fig. 8. Then, a 2×2 cm^2 buckling is placed on the disk. To detect the time related to the deformation, the sound condition signal is subtracted from the received defective signal.

Sampled received signal at the typical receiver has been shown in Fig. 9 (a). Fig. 9(a) shows the received signals by one of receiving antennas in sound and defective conditions of the transformer winding. Also, Fig. 9(b) shows the subtracted signal. In Fig. 9(b), T_C is the time interval of changes in the subtracted signal and as mentioned, it is related to the deformation distance from the antennas. As shown in Fig. 9(b), Tp is the time of subtracted signal peak. As regards in this paper, the cross-correlation method has been used to determine the time difference; the peak of subtracted signal is a good criterion.

In a real transformer, the propagation medium is oil. This will just affect the velocity of electromagnetic wave used in the denominator of equation (2), i.e. $v{=}3\times10^8/\sqrt{\varepsilon_r}\ m/s$ where ε_r is the relative dielectric constant of the oil. In a real transformer, the aging effect of the oil can be considered by regular measurements of the oil relative dielectric constant [22].

The initial tests show that the simulation results are close to the real space and experimental results. Fig. 10 depicts an experimental sample scan. It consists of three components, each associated with a path. The first part is the signal that travels directly from the TX to the RX, and is called crosstalk. The second part is the target's reflection, which is the desired signal. The third part, which is the reflections

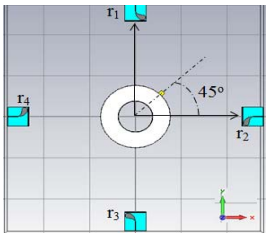

Fig. 11. Radial deformation location at 45 degree angle (top view).

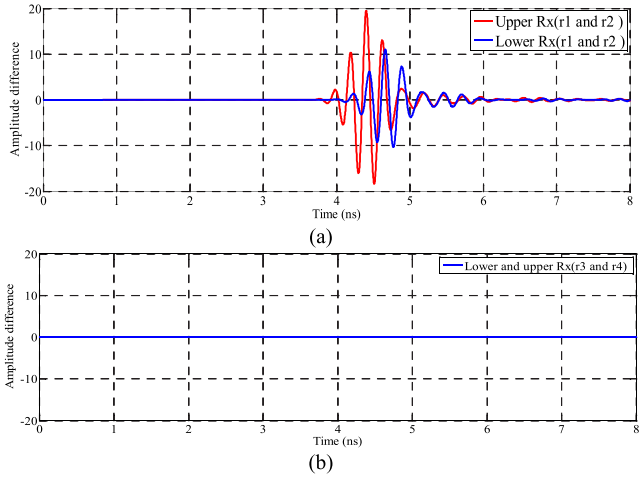

Fig. 12. Signals difference in normal and defected modes for radial deformation location at 45 degree angle for set of antennas (a) r_1 and r_2, and (b) r_3 and r_4.

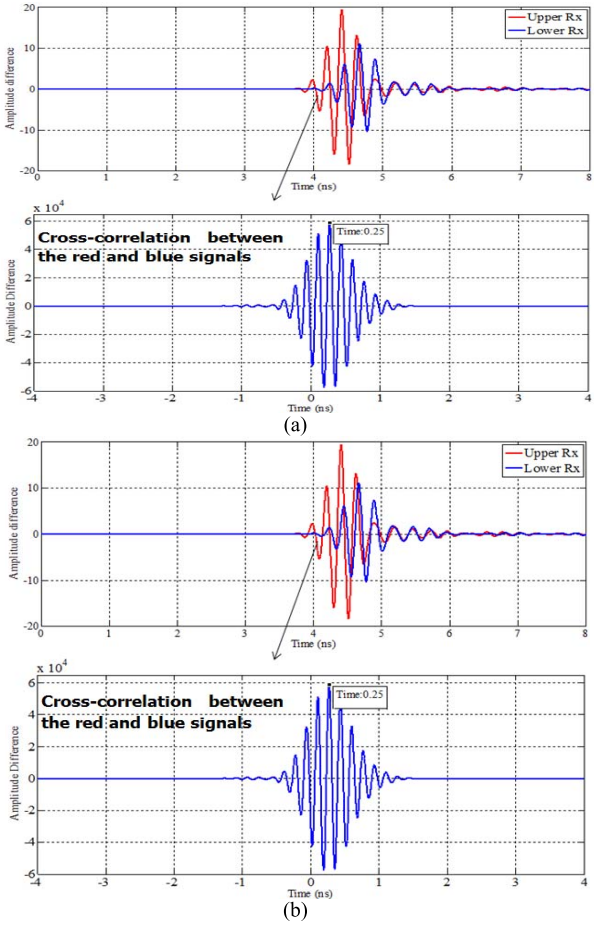

Fig. 13. Signals difference in normal and defected modes for radial deformation location at 45 degree angle. Antennas on (a) x=0 (r_1) and (b) y=0(r_2).

from other objects, is called ambient. In this experimental space, received signals show the environmental effects clearly. Comparing Fig. 9(a) and Fig. 10 depict that the first section of both received signals is similar but the last section (third section) of them which is the reflections from other objects is different. In the algorithm which is proposed in this paper, the signal of the sound condition is subtracted from the signal of the deformed condition and the final process is applied to these resulting subtracted signals, so these environmental reflections is removed and will not affect the result.

A. Radial Deformation Location at 45 Degree Angle

In this section, buckling is simulated at the point (*x=10.6cm, y=10.6cm, z=11.2cm*) at an angle of 45 degrees from the x-axis and height of 11.2 cm from the origin as shown in Fig. 11. In order to determine the quadrant in which the defection has been occurred, the results of subtracting signals in sound and faulty conditions for each set of antennas (shown by r_1, r_2, r_3 and r_4 in Fig. 11) are obtained and shown in Fig. 12. It is obvious from that only the sets of r_1 and r_2 can detect the defect. Thus, it can be inferred that the defection has occurred in the first quadrant.

Fig. 13 illustrates the result of subtracting signal in sound and faulty conditions for sets of antennas on the *x=0* and *y=0* (r_1 and r_2) respectively. In other words, Fig. 13 shows the amplitude difference of resultant signals for the upper and lower receiving antennas. The time difference between the subtracted signal peaks is shown in Fig. 13 which result from the implementation of the cross correlation.

According to Fig. 13(a), the time difference of the subtracted signal peaks from two receiving antennas on the *x=0* (r_1) is *0.25 ns*. This time difference has been calculated using cross correlation method exactly. From (2) it is obtained that:

$$x_1 - x_2 = 7.5cm \tag{9}$$

Similarly, from Fig. 13(b), the time difference of the subtracted signal peaks from two receiving antennas on the *y=0* (r_2) is *0.25 ns*. Consequently:

$$y_1 - y_2 = 7.5cm \tag{10}$$

where, y_1 and y_2 are the first and second receiving antennas distance from the defected part, respectively for antennas on the *y=0* (r_2). This means that $2a_0 = 7.5\ cm$ and $2a_1 = 7.5\ cm$. Thus, using (5), we have:

$$b_0^2 = c_0^2 = 15^2 - 3.75^2 = 274.94cm^2 \tag{11}$$

$$b_1^2 = c_1^2 = 15^2 - 3.75^2 = 274.94cm^2 \tag{12}$$

TABLE V
DEFORMATION LOCATION RESULTS

θ	$l_0(cm)$ $(x;y;z)$	Calculated Locations by (13), (14), (15), (16) and (17)				$l_1(cm)$ $(x;y;z)$	$e(cm)$
		$p_1(cm)$	$p_2(cm)$	$p_3(cm)$	$p_4(cm)$		
45°	(10.6;10.6;11.2)	(10.6;10.6;10.98)	(10.6;10.6;-10.98)	(-10.6;-10.6;15.49)	(-10.6;-10.6;-15.49)	(10.6;10.6;10.98)	0.22
30^0	(12.99;7.5;14.6)	(12.72;7.94;14.25)	(12.72;7.94;-14.25)	(-4.87;-14.18;-19.8)	(-4.87;-14.18;19.8)	(12.72;7.94;14.25)	0.62

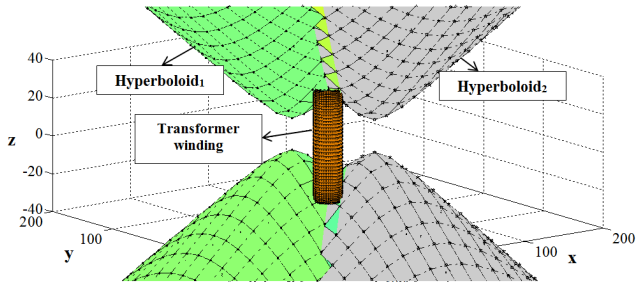

Fig. 14. Intersection of surfaces.

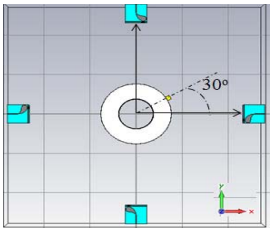

Fig. 15. Radial deformation location at 30 degree angle.

Adopting (6), (7), (8) and the corresponding parameters in Table IV, the following equations are derived:

$$x^2 + y^2 = 15^2 cm^2, \quad -30cm < z < +30cm \tag{13}$$

$$\frac{z^2}{3.75^2} - \frac{(x-55)^2}{16.58^2} - \frac{y^2}{16.58^2} = 1 \tag{14}$$

$$\frac{z^2}{3.75^2} - \frac{x^2}{16.58^2} - \frac{(y-55)^2}{16.58^2} = 1 \tag{15}$$

Fig. 14 shows the intersection of the above surfaces. By solving these equations, four points are obtained. As inferred from Fig. 12, the deformation is located in the first quadrant (i.e., *x, y>0*). Fig. 13 shows that upper antenna has observed the peak of subtracted signal amplitude (deformation) earlier than the lower one; so the point with positive z would be acceptable. All of the points calculated based on the simultaneous solution of equations, are listed in Table V.

B. Radial Deformation Location at 30 Degree Angle

In order to confirm the results of the previous section, the buckling is simulated at an angle of 30 degrees from the x-axis and height of *14.6 cm* (*x=12.99cm, y=7.5cm, z=14.6cm*) as shown in Fig. 15.

Similar to the previous section, the deformation location is detected by the subtraction of sound and deformed winding signals. As shown in Fig. 16, only the sets of antennas r_1 and r_2 have detected the defect, so it can be said that the defect is in the first quadrant.

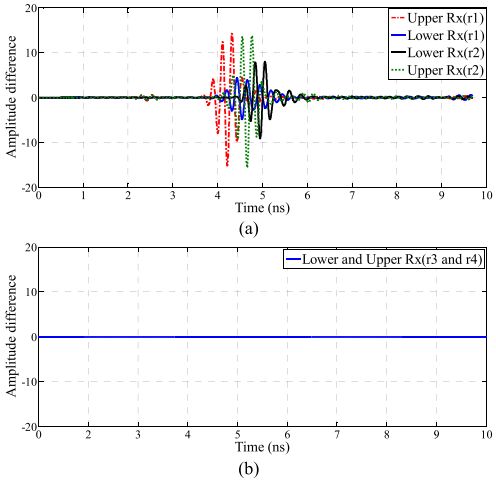

Fig. 16. Signals difference in normal and defected modes for radial deformation location at 30 degree angle for set of antennas: (a) r_1 and r_2 and (b) r_3 and r_4.

Fig. 17 shows the amplitude difference of resultant signals for sets of antennas r_1 and r_2, respectively. As shown in Fig. 17(a), the time difference of the subtracted signal peaks from two receiving antennas on the *x=0* (r_1) is *0.3 ns*. According to the Fig. 17 (b), this time difference for antennas on the *y=0* (r_2) is *0.27 ns*. Using (2), the following terms are calculated:

$$x_1 - x_2 = 9 \ cm \text{ and } y_1 - y_2 = 8.1 \ cm.$$

The new values of $2a_0$ and $2a_1$ would be *9cm* and *8.1cm*, respectively. Thus, using (5), we have:

$$b_0^2 = c_0^2 = 15^2 - 4.5^2 = 204.75cm^2 \text{ and}$$
$$b_1^2 = c_1^2 = 15^2 - 4.05^2 = 208.6cm^2.$$

Using (7), (8) and the new parameters, the following new surface equations representing the locus of the deformation are derived:

$$\frac{z^2}{4.5^2} - \frac{(x-55)^2}{14.31^2} - \frac{y^2}{14.31^2} = 1 \tag{16}$$

$$\frac{z^2}{4.05^2} - \frac{x^2}{14.443^2} - \frac{(y-55)^2}{14.443^2} = 1 \tag{17}$$

The exact location of the deformation is obtained using the intersection of these surfaces and the locus of the transformer winding model. The results are four points given in Table V, and only one point would be acceptable as discussed in previous subsection.

Table V gives radial deformation location results (obtained by simulation) and error percentage for deformation at two different locations. In this table, l_0 is actual coordinates of the

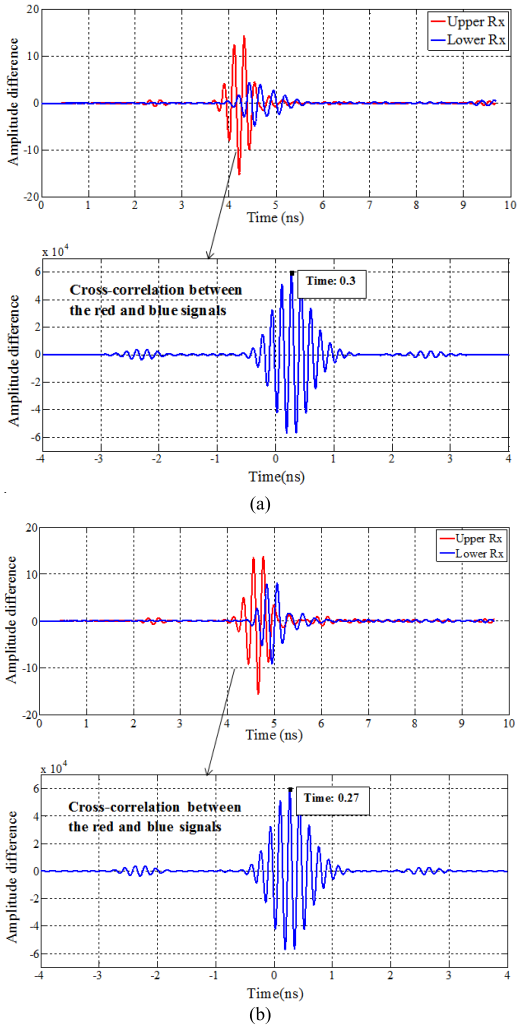

Fig. 17. Signals difference in normal and defected modes for radial deformation location at 30 degree angle. Antennas on: (a) x=0 (r_1) and (b) y=0 (r_2).

deformation location; p_1, p_2, p_3 and p_4 are the locations of the deformation determined by equations; l_1 and e are the location result and error, respectively, obtained by the proposed method of this paper and θ is the fault location angle from the *x-axis*.

The deformation location error defined as the distance between the actual and calculated location, is obtained as follows:

$$e = |l_1 - l_0| \tag{18}$$

As listed in Table V, the error of the presented method is very small. However, the results show that the proposed algorithm can efficiently detect the exact location of the deformation on the transformer winding.

VI. Conclusion

In this paper, a new on-line method has been proposed for the exact detection and localization of transformer winding radial deformation at the three-dimensional space. Based on the locus of objects in space, the UWB radar systems with four sets of antennas have been used for transmitting and receiving signals. To localize the winding deformation, first the sound condition signals for each set of antennas have been obtained using Vivaldi's antennas (in the time domain). Then, for faulty conditions, corresponding signals have been obtained and subtracted from the sound condition. The subtracted signals have been analyzed by using cross correlation method to exactly determine the defected location by solving and obtaining the intersection points of geometrical surfaces equations. The simulation results confirm the validity of the proposed algorithm.

References

[1] C. Bengtsson, "Status and trends in transformer monitoring," *IEEE Trans. Power Del.*, vol. 11, no. 3, pp. 1379–1384, Jul. 1996.

[2] H.-M. Ahn, Y.-H. Oh, J.-K. Kim, J.-S. Song, and S.-C. Hahn, "Experimental verification and finite element analysis of short-circuit electromagnetic force for dry-type transformer," *IEEE Trans. Magn.*, vol. 48, no. 2, pp. 819–822, Feb. 2012.

[3] E. Rahimpour, M. Jabbari, and S. Tenbohlen, "Mathematical comparison methods to assess transfer functions of transformers to detect different types of mechanical faults," *IEEE Trans. Power Del.*, vol. 25, no. 4, pp. 2544–2555, Oct. 2010.

[4] M. Steurer and K. Frohlich, "The impact of inrush currents on the mechanical stress of high voltage power transformer coils," *IEEE Trans. Power Del.*, vol. 17, no. 1, pp. 155–160, Jan. 2002.

[5] A. S. Morched, L. Marti, R. H. Brierley, and J. G. Lackey, "Analysis of internal winding stresses in EHV generator step-up transformer failures," *IEEE Trans. Power Del.*, vol. 11, no. 2, pp. 888–894, Apr. 1996.

[6] A. Bakshi and S. V. Kulkarni, "Eigenvalue analysis for investigation of tilting of transformer winding conductors under axial short-circuit forces," *IEEE Trans. Power Del.*, vol. 26, no. 4, pp. 2505–2512, Oct. 2011.

[7] T. De Rybel, A. Singh, J. A. Vandermaar, M. Wang, J. R. Marti, and K. D. Srivastava, "Apparatus for online power transformer winding monitoring using bushing tap injection," *IEEE Trans. Power Del.*, vol. 24, no. 3, pp. 996–1003, Jul. 2009.

[8] J. Christian and K. Feser, "Procedures for detecting winding displacements in power transformers by the transfer function method," *IEEE Trans. Power Del.*, vol. 19, no. 1, pp. 214–220, Jan. 2004.

[9] E. Rahimpour, J. Christian, K. Feser, and H. Mohseni, "Transfer function method to diagnose axial displacement and radial deformation of transformer windings," *IEEE Trans. Power Del.*, vol. 18, no. 2, pp. 493–505, Apr. 2003.

[10] T. Leibfried and K. Feser, "Monitoring of power transformers using the transfer function method," *IEEE Trans. Power Del.*, vol. 14, no. 4, pp. 1333–1341, Oct. 1999.

[11] A. Palani, S. Santhi, S. Gopalakrishna, and V. Jayashankar, "Real-time techniques to measure winding displacement in transformers during short-circuit tests," *IEEE Trans. Power Del.*, vol. 23, no. 2, pp. 726–732, Apr. 2008.

[12] J. Lu, J. Yuan, L. Chen, J. Sheng, and X. Ma, "Calculation of the short-circuit reactance of transformers by a line integral based on surface magnetic charges," *IEEE Trans. Magn.*, vol. 34, no. 5, pp. 3483–3486, Sep. 1998.

[13] D. K. Xu and Y. M. Li, "A simulating research on monitoring of winding deformation of power transformer by on-line measurement of short-circuit reactance," in *Proc. Conf. IEEE POWERCON*, vol. 1, Aug. 1998, pp. 167–171.

[14] T. Leibfried and K. Feser, "Off-line- and on-line-monitoring of power transformers using the transfer function method," in *Proc. Conf. Rec. IEEE Int. Symp. Elect. Insul.*, Montreal, QC, Canada, Jun. 1996, pp. 34–37.

[15] T. Leibfried and K. Feser, "On-line monitoring of transformers by means of the transfer function method," in *Proc. Conf. Rec. IEEE Int. Symp. Elect. Insul.*, Pittsburgh, PA, USA, Jun. 1994, pp. 111–114.

[16] M. Wang, A. J. Vandermaar, and K. D. Srivastava, "Condition monitoring of transformers in service by the low voltage impulse test method," in *Proc. 11th Int. Symp. High Voltage Eng.*, vol. 1. Aug. 1999, pp. 45–48.

[17] P. Gomez, F. de Leon, and I. A. Hernandez, "Impulse-response analysis of toroidal core distribution transformers for dielectric design," *IEEE Trans. Power Del.*, vol. 26, no. 2, pp. 1231–1238, Apr. 2011.

[18] A. Setayeshmehr, H. Borsi, E. Gockenbach, and I. Fofana, "On-line monitoring of transformer via transfer function," in *Proc. IEEE Elect. Insul. Conf. (EIC)*, May/Jun. 2009, pp. 278–282.

[19] M. Bagheri, M. S. Naderi, and T. Blackburn, "Advanced transformer winding deformation diagnosis: Moving from off-line to on-line," *IEEE Trans. Dielectr. Electr. Insul.*, vol. 19, no. 6, pp. 1860–1870, Dec. 2012.
[20] M. A. Hejazi, G. B. Gharehpetian, G. Moradi, H. A. Alehosseini, and M. Mohammadi, "Online monitoring of transformer winding axial displacement and its extent using scattering parameters and k-nearest neighbour method," *IET Generat., Transmiss. Distrib.*, vol. 5, no. 8, pp. 824–832, Aug. 2011.
[21] M. Akhavanhejazi, G. B. Gharehpetian, R. Faraji-Dana, G. R. Moradi, M. Mohammadi, and H. A. Alehoseini, "A new on-line monitoring method of transformer winding axial displacement based on measurement of scattering parameters and decision tree," *Expert Syst. Appl.*, vol. 38, no. 7, pp. 8886–8893, Jul. 2011.
[22] M. S. A. Hejazi, J. Ebrahimi, G. B. Gharehpetian, M. Mohammadi, R. Faraji-Dana, and G. Moradi, "Application of ultra-wideband sensors for on-line monitoring of transformer winding radial deformations—A feasibility study," *IEEE Sensors J.*, vol. 12, no. 6, pp. 1649–1659, Jun. 2012.
[23] M. S. Golsorkhi, M. S. A. Hejazi, G. B. Gharehpetian, and M. Dehmollaian, "A feasibility study on the application of radar imaging for the detection of transformer winding radial deformation," *IEEE Trans. Power Del.*, vol. 27, no. 4, pp. 2113–2121, Oct. 2012.
[24] P. Karimifard and G. B. Gharehpetian, "A new algorithm for localization of radial deformation and determination of deformation extent in transformer windings," *Electr. Power Syst. Res.*, vol. 78, no. 10, pp. 1701–1711, Oct. 2008.
[25] K. Ragavan and L. Satish, "Localization of changes in a model winding based on terminal measurements: Experimental study," *IEEE Trans. Power Del.*, vol. 22, no. 3, pp. 1557–1565, Jul. 2007.
[26] L. Satish and S. K. Sahoo, "Locating faults in a transformer winding: An experimental study," *Electr. Power Syst. Res.*, vol. 79, no. 1, pp. 89–97, Jan. 2009.
[27] S. Pramanik and L. Satish, "Localisation of discrete change in a transformer winding: A network-function-loci approach," *IET Electr., Power. Appl.*, vol. 5, no. 6, pp. 540–548, Jul. 2011.
[28] F. C. Commission, "Revision of part 15 of the commission's rules regarding ultra-wideband transmission," Federal Commun. Commission, Washington, DC, USA, Tech. Rep. 98-153, Apr. 2002.
[29] H. Rahbarimagham, M. A. Hejazi, H. K. Porzani, M. S. Naderi, and G. B. Gharehpetian, "Exact determination of a winding disk radial deformation location considering tank effect using an analytical method," in *Proc. 21st Iranian Conf. Elect. Eng. (ICEE)*, Mashhad, Iran, May 2013, pp. 1–5.
[30] H. Rahbarimagham, M. S. Naderi, G. B. Gharehpetian, M. A. Hejazi, and H. K. Porzani, "A novel method for exact determination to localize radial deformation along the transformer winding height," in *Proc. 4th Conf. Thermal Power Plants (CTPP)*, Tehran, Iran, Dec. 2012, pp. 1–5.
[31] R. S. Thoma, O. Hirsch, J. Sachs, and R. Zetik, "UWB sensor networks for position location and imaging of objects and environments," in *Proc. EUCAP*, Nov. 2007, pp. 1–9.
[32] A. H. Sayed, A. Tarighat, and N. Khajehnouri, "Network-based wireless location: Challenges faced in developing techniques for accurate wireless location information," *IEEE Signal Process. Mag.*, vol. 22, no. 4, pp. 24–40, Jul. 2005.
[33] N. Patwari, J. N. Ash, S. Kyperountas, A. O. Hero, R. L. Moses, and N. S. Correal, "Locating the nodes: Cooperative localization in wireless sensor networks," *IEEE Signal Process. Mag.*, vol. 22, no. 4, pp. 54–69, Jul. 2005.
[34] S. Gezici *et al.*, "Localization via ultra-wideband radios: A look at positioning aspects for future sensor networks," *IEEE Signal Process. Mag.*, vol. 22, no. 4, pp. 70–84, Jul. 2005.
[35] B. Friedlander, "A passive localization algorithm and its accuracy analysis," *IEEE J. Ocean. Eng.*, vol. 12, no. 1, pp. 234–245, Jan. 1987.
[36] K. Yu, J.-P. Montillet, A. Rabbachin, P. Cheong, and I. Oppermann, "UWB location and tracking for wireless embedded networks," *Signal Process.*, vol. 86, no. 9, pp. 2153–2171, Sep. 2006.
[37] Y. Norouzi and M. Derakhshani, "Joint time difference of arrival/angle of arrival position finding in passive radar," *IET Radar, Sonar Navigat.*, vol. 3, no. 2, pp. 167–176, Apr. 2009.
[38] O. Javashvili, "UWB antennas for wall penetrating radar systems," M.S. thesis, Dept. Technol. Built Environ., Gävle Univ., Gävle, Sweden, 2009.
[39] A. Mehdipour, K. Mohammadpour-Aghdam, and R. Faraji-Dana, "Complete dispersion analysis of Vivaldi antenna for ultra wideband applications," *Prog. Electromagn. Res.*, vol. 77, 2007, pp. 85–96.

Hesam Rahbarimagham received the B.Sc. degree in electrical engineering from the Shiraz University of Technology, Shiraz, Iran, in 2011. He is currently pursuing the M.Sc. degree in electrical engineering at the Amirkabir University of Technology, Tehran, Iran. His research interests include power system and power transformer monitoring, HVdc transmission systems, and microgrids.

Hossein Karami Porzani was born in Isfahan, Iran, in 1988. He received the B.Sc. and M.Sc. degrees in electrical engineering from the Amirkabir University of Technology, Tehran, Iran, in 2010 and 2012, respectively, where he is currently pursuing the Ph.D. degree. His research interests are smart home, distributed generation in power systems, and partial discharge in power transformers.

Maryam Sadat Akhavan Hejazi received the B.Sc. degree in electrical engineering, in 2003, and the M.Sc. and Ph.D. degrees in electric power engineering from the Amirkabir University of Technology, Tehran, Iran, in 2006 and 2011, respectively. She is currently an Assistant Professor with the University of Kashan, Kashan, Iran. She has authored over 30 journal and conference papers. Her research interests include transformer monitoring and modeling, distributed generation, and smart grid.

Mahdi S. Naderi was born in Tabriz in 1976. He received the B.S. degree in electrical engineering from the Sharif University of Technology, Tehran, Iran, in 1998, and the M.S. and Ph.D. degrees in electrical engineering from the Amirkabir University of Technology (AUT), Tehran, in 2001 and 2007, respectively. He has been with the School of Electrical Engineering and Telecommunication, University of New South Wales, Sydney, Australia. He has also been an Assistant Professor with the Iran Grid Secure Operation Research Center, AUT, since 2008. His teaching and research interests include network planning, power system and transformers transients, FACTS devices, distributed generation, and HVdc transmission systems. He is a member of the Iranian Association of Electrical and Electronics Engineers and the Engineers Australia. As a Ph.D. student, he received a scholarship from Iran Power Generation, Transmission and Distribution Management Company (Tavanir) from 2005 to 2006.

Gevork B. Gharehpetian received the Ph.D. (Hons.) degree in electrical engineering from the University of Tehran, Tehran, Iran, in 1996.

He was an Assistant Professor with the Amirkabir University of Technology, Tehran, from 1997 to 2003, and an Associate Professor from 2004 to 2007. He has been a Professor since 2007. He has authored over 750 journal and conference papers. His teaching and research interests include power system and transformers transients and power-electronics applications in power systems.

Prof. Gharehpetian is a Senior Member and Distinguished Member of the Iranian Association of Electrical and Electronics Engineers (IAEEE), respectively, and a member of the Central Board of IAEEE. He received the National Prize in 2008 and 2010, respectively. He was selected by the Ministry of Higher Education as a Distinguished Professor of Iran and the IAEEE as a Distinguished Researcher of Iran.